

Reliability in Semantic Segmentation: Can We Use Synthetic Data?

Thibaut Loiseau^{2,†} Tuan-Hung Vu¹ Mickael Chen¹ Patrick Pérez¹ Matthieu Cord^{1,3}
¹Valeo.ai ²ENPC ParisTech ³Sorbonne University

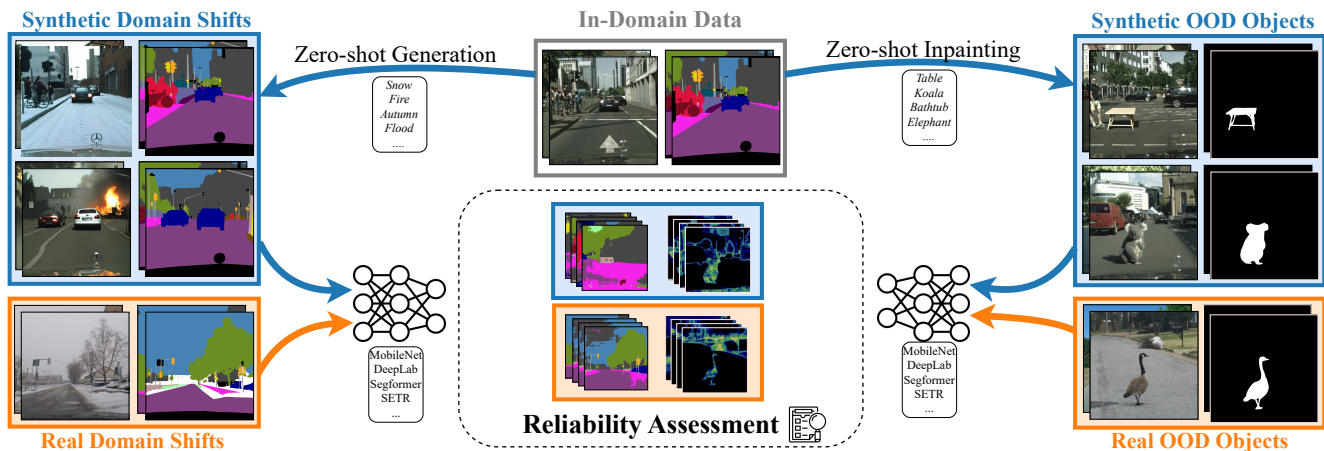


Figure 1. **An overview of our study.** Starting with in-domain data, we generate synthetic samples with the required ground truths for metrics computation. The quantitative comparison involves synthetic data vs. real data with various domain shifts and OOD objects.

Abstract

Assessing the reliability of perception models to covariate shifts and out-of-distribution (OOD) detection is crucial for safety-critical applications such as autonomous vehicles. By nature of the task, however, the relevant data is difficult to collect and annotate. In this paper, we challenge cutting-edge generative models to automatically synthesize data for assessing reliability in semantic segmentation. By fine-tuning Stable Diffusion [27], we perform zero-shot generation of synthetic data in OOD domains or inpainted with OOD objects. Synthetic data is employed to provide an initial assessment of pretrained segmenters, thereby offering insights into their performance when confronted with real edge cases. Through extensive experiments, we demonstrate a high correlation between the performance on synthetic data and the performance on real OOD data, showing the validity approach. Furthermore, we illustrate how synthetic data can be utilized to enhance the calibration and OOD detection capabilities of segmenters.

1. Introduction

Fueled by extensive training data, modern neural networks consistently advance accuracy across various percep-

tion benchmarks. Despite the rapid adoption of deep networks in safety-critical applications, reliability [23, 31, 33] has been an overlooked factor when designing and training these models. Recent efforts are geared toward enhancing model robustness under covariate shifts in data distributions [23, 26] and improving the model’s ability to detect the *unknown* [10, 11, 36]. For open-world validation, in-domain data is no longer sufficient [14]; reliable and trustworthy systems demand more rigorous testing on diverse distributions, potentially exhibiting unknown objects. However, collecting and annotating data is a challenging and costly endeavor. Data collection campaigns can be quickly overwhelmed by the growing number of out-of-distribution (OOD) conditions and objects.

While real data remains the ultimate resource for validating real-world applications, recent advances in generative networks bring hopes for a potential automatic validation framework that can gradually alleviate the need for collecting and annotating real data [17, 25]. Trained on massive datasets, state-of-the-art generative networks are regarded as foundation generalists that encompass vast semantic and domain knowledge. Furthermore, text-to-image models like Stable Diffusion [27], empowered by large vision-language models, possess the seamless prompting ability that enables zero-shot generation. Via prompting, one can intentionally generate data from any target domain with minimal ef-

[†]This work was done during an internship at Valeo.ai

fort, allowing stress-testing perception models even under extremely rare conditions. For instance, although fires or floods rarely occur in reality, self-driving cars are deemed robust and resilient; testing in such conditions is therefore crucial. Moreover, in the open world, objects not encountered during training may appear anywhere; a reliable system should be capable of recognizing its limitations and classifying such objects as *unknown*, referred to as OOD detection. Recent OOD detection datasets attempt to benchmark perception models with random objects found on the road [3, 4, 12, 24]; however, the number of test images and the variety of OOD objects are very limited. To tackle this challenge cost-effectively, zero-shot generative inpainting emerges as a promising tool, enabling validation across a much wider range of objects.

In this work, we exploit generative networks as a general validator, targeting multiple faces of reliability. We benchmark segmentation robustness under global covariate shifts and the ability to locally detect OOD objects. Further than that, our synthetic data can be used for calibrating pretrained models to targeted domains and for improving the OOD detection performance. To validate our proposal, we compare our synthetic data against using real test data from existing benchmarks on similar tasks, i.e. ACDC [28] and SegmentMeIfYouCan [4]. Extensive experiments demonstrate our findings as follows:

- Synthetic data can serve as a reliable indicator of the real-life performance of segmenters under covariate shifts.
- Pretrained segmenters can leverage synthetic data to improve confidence calibration.
- Synthetic inpainted data is valuable for benchmarking OOD detection. Our high-quality synthetic data is featured in the official BRAVO benchmark.¹
- Training on inpainted OOD objects helps models become more discerning when encountering real OOD objects.

2. Related Work

Covariate Shifts. Modern machine learning models, notably deep networks, fall short in preserving their robustness and estimating their prediction confidence in the presence of covariate shifts [23, 26]. The last few years have witnessed the emergence of various benchmarks [6, 9, 14, 30, 31] that address the need for assessing models’ reliability under different distributional shifts. Hendrycks et al. [9] propose a pioneering benchmark featuring data corrupted by various synthetic perturbations such as noise, blur, and brightness,

¹<https://valeoai.github.io/bravo/>

etc. Taori et al. [31] emphasize the importance of realistic shifts in reliability assessment; they highlight the disparity between natural and synthetic shifts, asserting that there is minimal to no robustness transfer from synthetic to natural distribution shifts. Sign et al. [30] study low-shot robustness to natural distribution shifts, highlighting the robustness properties of advanced architecture and pretraining strategies. In [5], de Jorge et al. extend beyond the standard classification setup to address the reliability problem in semantic segmentation. Most findings are largely aligned with previous works on classification; one interesting finding is on the disconnection between robustness and confidence calibration, urging more attention to calibration during segmenter design and training. On the same research line, one intriguing aspect is to study the connections between in-domain and out-of-domain robustness [5, 21, 32]; different findings suggest either positive, none or even negative correlations between ID and OOD robustness, which indeed largely depends on the type of shifts. In line with [5], we focus on segmentation as the primary research task. Different from previous works, we advocate for the use of advanced generative models to generate realistic synthetic data for testing segmenters under arbitrary covariate shifts. We align with [31] regarding the realism of testing data and argue for the rapid maturation of generative models that are progressively narrowing the gap between synthetic and real shifts. Our goal is to study whether synthetic data can be a superior choice compared to ID data in correlation studies against OOD robustness – referred to as real-shift robustness in the subsequent text to avoid confusion with OOD detection. Motivated by [5], we also attempt to address the calibration problem by leveraging our synthetic data.

OOD Object Detection. In addition to robustness and calibration, the ability to detect the “unknown” is an equally important aspect, completing the reliability assessment for trustworthy systems [10, 11, 36]. In semantic segmentation, several datasets are available for evaluating OOD detection on the road, namely LostAndFound [24], StreetHazards [12] (synthetic), BDD-Anomaly [12], Fishyscapes [3] (synthetic) and SegmentMeIfYouCan [4]. Encountering and capturing images of OOD objects in real-world scenarios, without deliberately placing objects on the road, is quite uncommon. Effectively, existing datasets are limited in scale, both in terms of the number of images and the variety of object classes. In this work, we propose leveraging advanced zero-shot inpainting techniques to augment an existing segmentation dataset with inpainted OOD objects; enabling the generation of highly realistic synthetic data for testing and training OOD detection.

Synthetic Data for Testing. Generative models have been exploited to generate training data either for image classification [2, 8, 29], object detection [20], or semantic segmentation [15, 16, 35, 38]. Only recently, a few works

have delved into the topic of generative testing data. Li et al. [17] exploit diffusion models to realistically edit images, controlling over various object attributes. This approach enables stress-testing models and understanding their sensitivity to different attributes. Using Stable Diffusion, LANCE [25] generates counterfactual images capable of challenging any given perception model. To the extent of our knowledge, no existing works have proposed to generate testing data for segmentation reliability.

3. Reliability Under Covariate Shifts

In this section, we explore whether synthetic data can be used to assess the robustness of pretrained segmenters in the presence of covariate shifts to unseen domains. We describe the data generation process and present the benchmarking results for a wide range of segmenters on our synthetic data.

3.1. Generating images in arbitrary domains

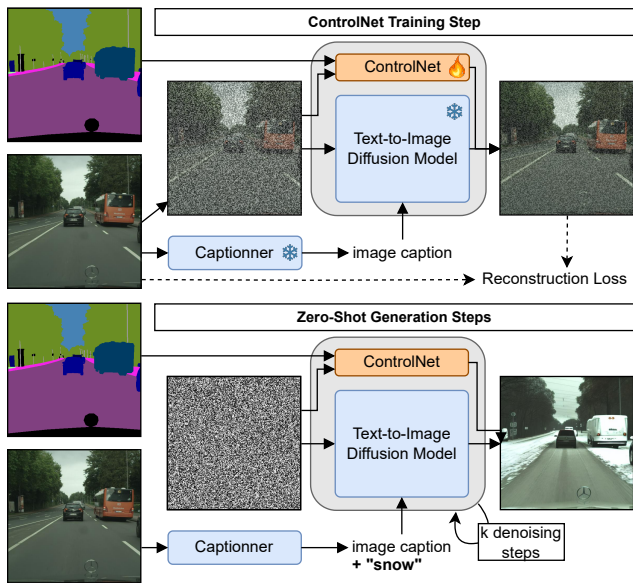


Figure 2. **Generating data with covariate shifts.** Training (top) and Sampling (bottom) processes for producing the synthetic data with shifts. Note that we only use images and labels from the original domain.

Our goal here is to obtain pairs of images and semantic masks, with the images belonging to visual domains for which we lack data. To this end, we leverage a pretrained text-to-image Stable Diffusion (SD) model [27], repurposed as a semantic conditioned model called ControlNet [37]. The ControlNet is trained solely on images and segmentation ground truths from the Cityscapes dataset; at train time, the text prompts are captions automatically extracted using CLIP-interrogator [1]. As a result, the model is able to perform mask-to-image generation of driving scenes while

retaining the ability to steer the generation through text prompting of Stable Diffusion.

To generate synthetic data, we prompt the trained ControlNet by the concatenation of target domain descriptions and CLIP-interrogator captions obtained from Cityscapes validation images. Also, segmentation masks in the Cityscapes validation set are used to condition the generative process. Thanks to zero-shot prompting, the synthetic images are aligned with the semantic condition while displaying the visual properties of arbitrary target domains. Figure 2 illustrates the training and generation steps. Detailed technical descriptions and more visualizations are in Appendix A.

3.2. Robustness Assessment with Synthetic Data

With the pipeline outlined in Section 3.1, one can generate synthetic data to assess the robustness of pretrained segmenters in any target unseen domains through zero-shot prompting. To quantify robustness, we employ the traditional mean Intersection-over-Union (mIoU) score, measuring the correct overlap between semantic predictions and ground-truth masks. Given that our synthetic dataset comprises pairs of segmentation masks and synthetic images, one can straightforwardly derive synthetic scores for any pretrained segmenters. We here investigate whether synthetic performance can comparatively reflect the performance on real data in target domains under covariate shifts.

Experimental Setups. We address weather shifts and geographical shifts, which are often encountered in the context of autonomous driving. These covariate shifts are exhibited in the two existing real datasets: the Adverse Conditions Dataset (ACDC) [28] and the Indian Driving Dataset (IDD) [34]. We utilize those real data to quantify the quality of our synthetic data and to validate its usefulness.

Synthetic data are generated by conditioning on semantic masks from the Cityscapes validation set. To prompt the ControlNet, we concatenate CLIP-interrogator’s caption with domain description following a simple template [`<caption>`, `in <domain>`] where domain is either ‘india’, ‘fog’, ‘rain’, ‘snow’ or ‘night’.

For testing, we gather a collection of 40 publicly available segmenters trained *only on Cityscapes*, representatives of a variety of backbones, segmentation architectures, and network sizes. The full list of models is in Appendix A.

Results. In Figure 3, we present our main results of this study. Our primary metric is the Pearson Correlation Coefficient (PCC) between the mIoUs on testing data *vs.* the mIoUs on real-shift data from ACDC’s splits or IDD. The testing data can be either the Cityscapes validation set (CS) or our synthetic data (syn); the idea is to see which testing data –whether real CS or our synthetic– correlates more with the real-shift data.

We organize our results based on increasing domain gaps

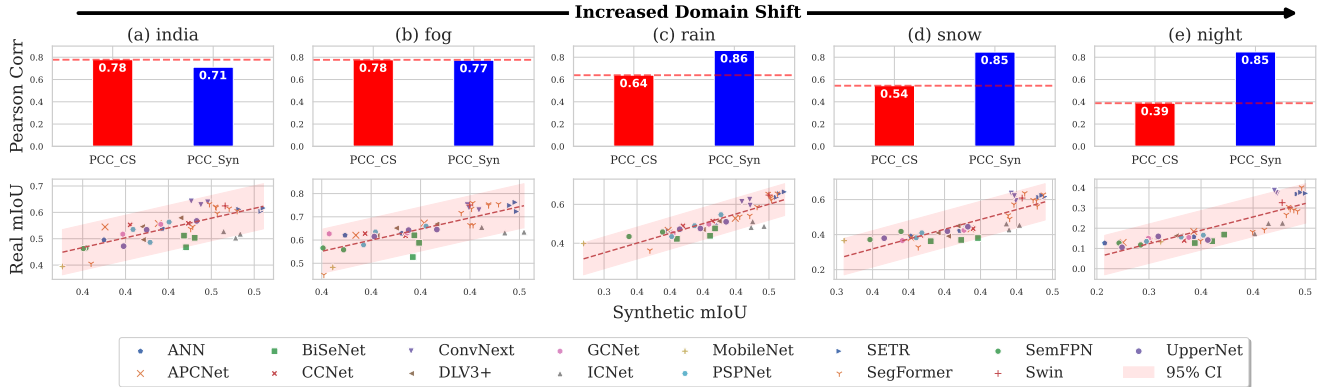


Figure 3. **Robustness Correlation** on real vs. synthetic covariate shifts across 40 pretrained segmenters with different architectures and network sizes. Each subplot in the second row displays the scattered mIoUs (synthetic vs. real) and the linear regression line accompanied by 95% confidence intervals (CI). The subplots in the top row illustrate the Pearson Correlation Coefficients, (i) between Cityscapes mIoUs vs. real-shift mIoUs (PCC_CS ■), as well as (ii) between synthetic-shift mIoUs vs. real-shift mIoUs (PCC_Syn ■). The subplots are sorted from left to right based on domain gaps to Cityscapes, represented by PCC_CS (■). The robustness results on synthetic data exhibit a strong correlation with those on real data, particularly in the case of the most distant shifts like ‘snow’ and ‘night’.

relative to the Cityscapes domain. The domain gaps are quantified by the Pearson correlation between Cityscapes mIoUs and real-shift mIoUs, annotated as PCC_CS and visualized as red bars ■ in the subplots of Figure 3. Moving from left to right, *i.e.* with growing domain gaps, we observe a widening discrepancy between PCC_CS and PCC_Syn. Here, PCC_Syn (■) represents the Pearson correlation between synthetic mIoUs and real-shift mIoUs. In domains with small gaps, PCC_CS and PCC_Syn are relatively comparable. However, in domains with more adverse shifts, such as ‘snow’ and ‘night’, PCC_Syn outperforms PCC_CS significantly, exceeding PCC_CS in ‘night’ by more than double.

In Figure 4, we analyze the results for the ‘night’ condition using the most robust models across different architectures, ranging from traditional convnets to recent transformer networks. We use the Semantic-FPN score as the reference to normalize the scores of other models. This normalization aims to illustrate the relative improvement in robustness concerning architecture. We rank the models from left to right based on their performance on real night data from the ACDC-night split. The consistently increasing trend of synthetic scores (■) from left to right demonstrates a strong correlation with the ranking based on real scores. Conversely, Cityscapes scores (■) are not indicative of night performance; that is, a higher mIoU obtained on Cityscapes does not immediately translate into a higher mIoU at night.

Since synthetic data can be generated in any desired quantity, a natural question arises: how many images are sufficient? In addressing this question, we conducted experiments and presented the results in Figure 5. Our empirical finding suggests that ~ 500 synthetic images are adequate for a stable and reliable assessment of robustness.

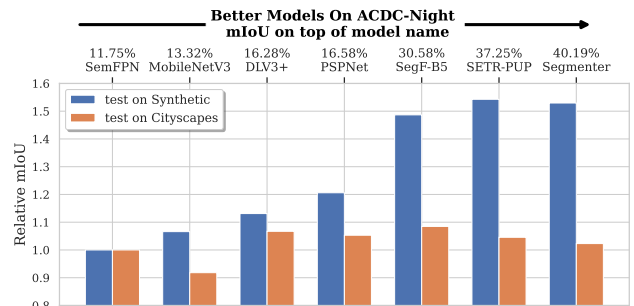


Figure 4. **Day-night shift.** Models are ranked from left to right by their robustness on real night data – ACDC-Night mIoUs are shown on top of model names. For each presented architecture, the most robust model on Cityscapes is tested; the Semantic-FPN, DeeplabV3+, and PSPNet models have ResNet-101 as backbone. The Semantic-FPN model (lowest mIoU on ACDC-Night) serves as the reference for computing the relative mIoUs. Blue bars or orange bars show the relative mIoUs when testing on our synthetic data (■) or testing on Cityscapes validation data (■). Cityscapes scores are not reliable for ranking models in the night domain. Synthetic scores exhibit a stronger correlation with real night scores, as evidenced by the more consistently increasing trend in the blue bars from left to right.

Discussion. In the recent work on reliability in semantic segmentation [5], Jorge et al. systematically quantified the robustness of segmenters on real-shift data; similarly to ours, they draw comparisons from ACDC and IDD datasets. One intriguing finding in this paper is that “..the larger the domain shift, the larger the improvement brought by more recent segmentation models”, hinting at a correlation between model robustness on in-domain data and covariate-shift data. In our study, we delve deeper into this correlation, choosing to separately address different weather types

instead of grouping them all together as done in [5]. In domains exhibiting small gaps to Cityscapes, such as IDD or ACDC-Fog, our conclusion aligns with [5]. However, as domain gaps increase, the discrepancy between Cityscapes mIoUs and real-shift mIoUs becomes more pronounced, resulting in poor PCC_CS scores. On the contrary, synthetic mIoUs and real-shift mIoUs exhibit a strong correlation across shifts. *Our empirical study has validated that synthetic performance is a reliable indicator of model robustness in the presence of covariate shifts.*

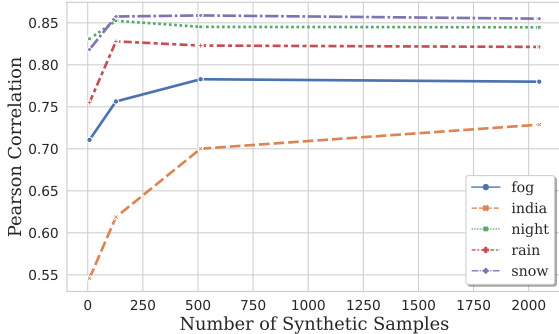


Figure 5. **Pearson Correlation vs. # Synthetic Samples.** The use of more synthetic samples contributes to increased stability in the results. Empirical plots demonstrate that approximately 500 samples are sufficient for a stable correlation assessment.

3.3. Confidence Calibration with Synthetic Data

Confidence calibration is a crucial aspect of deep networks, particularly when employed in safety-critical applications such as autonomous driving. Jorge et al. [5] highlighted a disconnection between model robustness and calibration, asserting that “... despite the remarkable improvements in terms of robustness, recent models are not significantly better calibrated”. Therefore, it is essential to devise techniques and protocols for recalibrating data, particularly in domains exhibiting covariate shifts. Drawing inspiration from this, we explore the feasibility of using synthetic data to recalibrate pretrained segmenters.

We perform temperature scaling using our synthetic data. Temperature scaling [7] is a well-established technique for calibrating pretrained models, typically conducted on a small validation set within the target domain. In our study, for each segmenter, we utilized the same sets of synthetic data generated in Section 3.2 to optimize temperature scaling factors, with one adjustment made for each covariate shift. For comparison, we replicate the process using real-shift data from ACDC and IDD.

Figure 6 reports the calibration improvement for the 40 pretrained segmenters using either real-shift data (orange bar) or synthetic data (blue bar). The subplots are arranged in increasing domain gap order from top to bottom, with the segmenters ranked from left to right based on increasing robustness

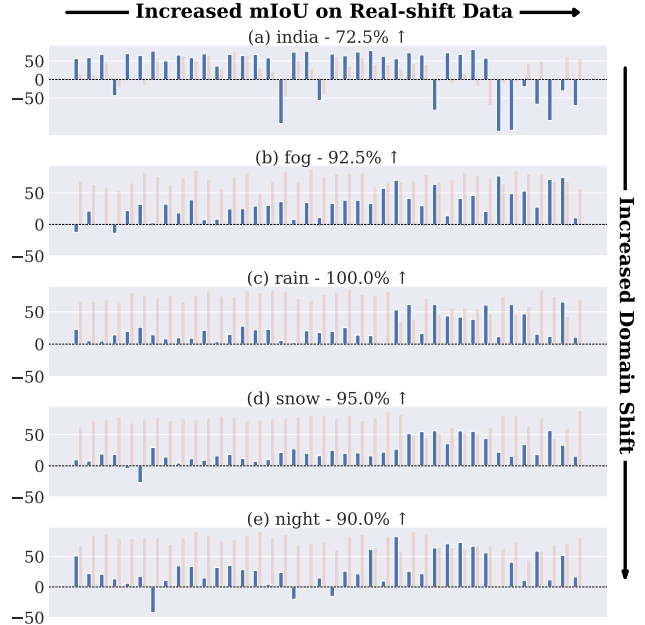


Figure 6. **ECE improvement using synthetic data.** The 40 segmenters are calibrated using either real-shift data or synthetic data. For each model, the relative ECE improvement (%) over its non-calibrated version is computed, visualized by blue (synthetic shift) and orange (real shift). The subplots are ranked by model robustness on real-shift data (left-to-right) and by the increased domain shift (top-to-bottom). The improvements in calibration are observed when using synthetic data, although those are much less pronounced compared to when using real data. The titles of the subplots indicate the percentage of models that showed improvement with synthetic data. In the case of weather shifts, we observe that synthetic data is particularly helpful for more robust models (i.e., the right part), while for geographical shifts, the improvement is more significant for the least robust models.

on real-shift data. The Expected Calibration Error (ECE) quantifies the calibration results, with a lower ECE indicating a better-calibrated model. For better visualization and interpretation, we present the relative ECE improvement and interpretation, computed as the percentage decrease in ECE after calibration compared to the original ECE without calibration. For example, a model with an ECE of 0.4 before calibration and an ECE of 0.2 after calibration will achieve a $(0.4 - 0.2)/0.4 = 50\%$ relative improvement.

We observe promising calibration results when employing our synthetic data. While not as good as real-shift data, synthetic data achieves a promising success rate of 72.5% on IDD and exceeds 90% on the four ACDC shifts. Interestingly, in weather shifts, we empirically observe that more robust models derive greater benefits when calibrated using our synthetic data; the reverse is observed for ‘europe-india’ geographical shift. While with real-shift data, robustness and calibration are not well correlated [5], our results suggest that a potential correlation might exist between the

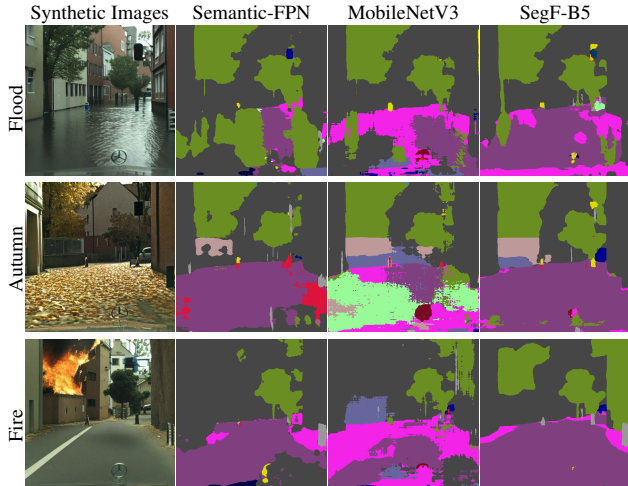


Figure 7. **Qualitative results.** Examples of rare conditions generated for testing and predictions from different models. Results of the strong model like SegFormer-B5 is visibly better than the Semantic-FPN and MobileNetV3.

two factors when using synthetic data. In [Appendix B](#), we provide technical details on our calibration approaches and additional results.

3.4. On Practical Applicability

One significant advantage of our framework lies in its potential to address rare conditions simply through prompting. The practical applicability of generative testing is tremendous. Our results demonstrate promising signals; practitioners can begin assessing and ranking their pre-trained models for a new, unseen target domain of interest *without the need for real data collection*. In practice, our proposed generative benchmarking can serve as the initial step in a full validation pipeline, helping filter out non-robust prototypes and thereby saving on total operational costs. Starting from complementing real-data validation, one can envision a future where generative techniques mature to the point of fully replacing real-data validation. In [Figure 7](#), we visualize some synthetic images and model predictions under rare conditions, such as being flooded with water, having autumn leaves scattered across the road, or having a building on fire. We observe clear visual distinctions between weaker (Semantic-FPN and MobileNetV3) and stronger (SegF-B5) models, knowing that their Cityscapes scores do not differ significantly. More examples are provided in [Appendix C](#).

4. Reliability Against OOD Objects

We now address the reliability of segmentation models in the presence of Out-of-Distribution (OOD) objects. To begin, we explain our pipeline for inpainting random OOD objects into existing Cityscapes images. Following that, we

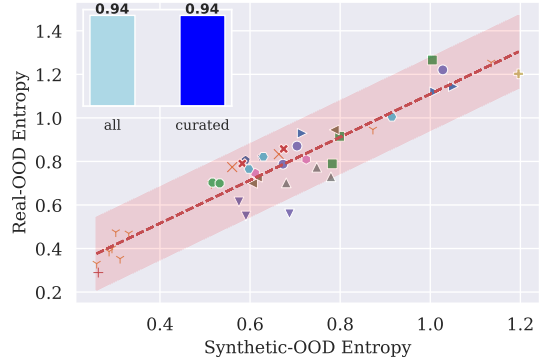


Figure 8. **Entropy Correlation.** The top-left inset reports the Pearson correlations between real-OOD entropy vs. synthetic-OOD entropy, computed either on ‘curated’ (■) or all synthetic inpainted images (●). Evaluations are performed on the same model set used in [Figure 3](#), with similar markers.

demonstrate how one can utilize inpainted images for OOD detection assessment and for enhancing OOD detection.

4.1. Inpainting Anomaly Objects

We inpaint random objects into Cityscapes images. To this end, we initially sample a location — a square box to which we inpaint the new object. We crop the box, up-sample its content to match the preferred output size of the generative model, and inpaint an object guided by a text prompt. In this step, we leverage Stable Diffusion inpainting capabilities, obtaining high-definition square images of the desired object. This image is then resized and pasted back into the original image, creating a final high-definition synthetic image. To ensure compositional consistency, we employ two techniques: Firstly, we divide the cropped box into two regions by center cropping it again. We inpaint only the inner region, leaving the outer region untouched, similar to the approach in RePaint [19]. Secondly, after composing the final image, we address any remaining inconsistencies by applying a light noise over the entire picture and performing reverse diffusion again. Technical details and visualizations are provided in [Appendix A](#).

After inpainting, it is necessary to extract the mask corresponding to the new object. To achieve this, we begin with a high-definition square image and apply the Grounded Segment Anything [13, 18], prompted with the name of the object. This process yields a mask within the square image, which can then be repositioned in the full image.

Our end-to-end generation pipeline is fully automatic. Through qualitative assessment, we achieve a satisfactory success rate in terms of generation realism; some inpainted images are illustrated in [Figure 10](#) and much more in [Appendix C](#). However, this still leaves a few generations with artifacts, characterized by either unusual compositions or unrealistic details. *We here question the criticality of realism in assessing OOD detection and, furthermore, in im-*

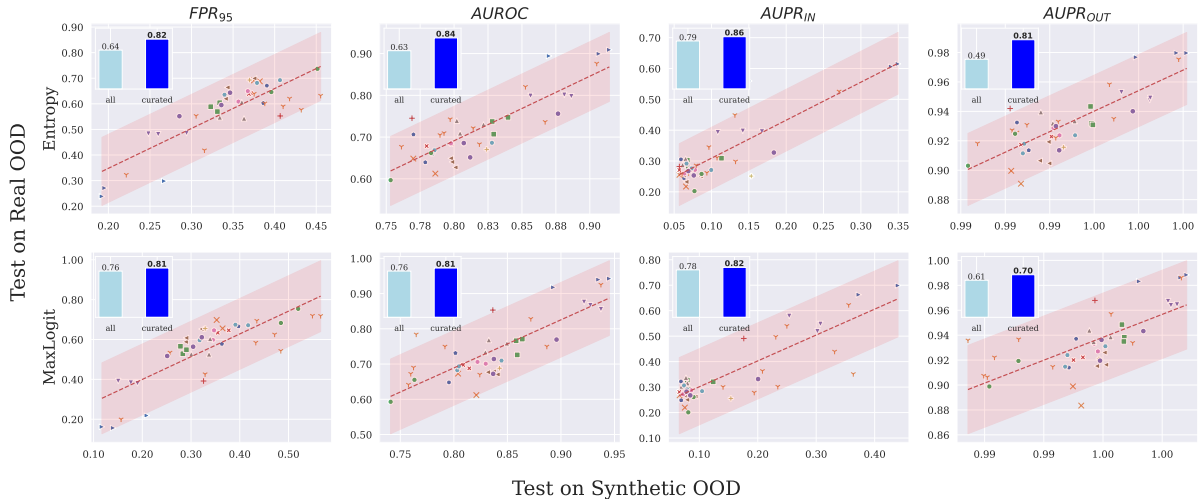


Figure 9. **Correlation in OOD Detection.** Each subplot scatters computed anomaly scores of segmenters on real OODs (y-axis) and on synthetic OODs (x-axis). The top row shows the four anomaly metrics utilized: FPR_{95} , AUROC, $AUPR_{IN}$, and $AUPR_{OUT}$. The results are organized into two rows corresponding to two different confidence measures (i) Entropy and (ii) MaxLogit. In the top-left corner of each subplot, an inset plots Pearson correlations to real OOD for ‘curated’ (■) and ‘all’ (□) synthetic sets. Evaluations are performed on the same model set used in Figure 3, with similar markers.

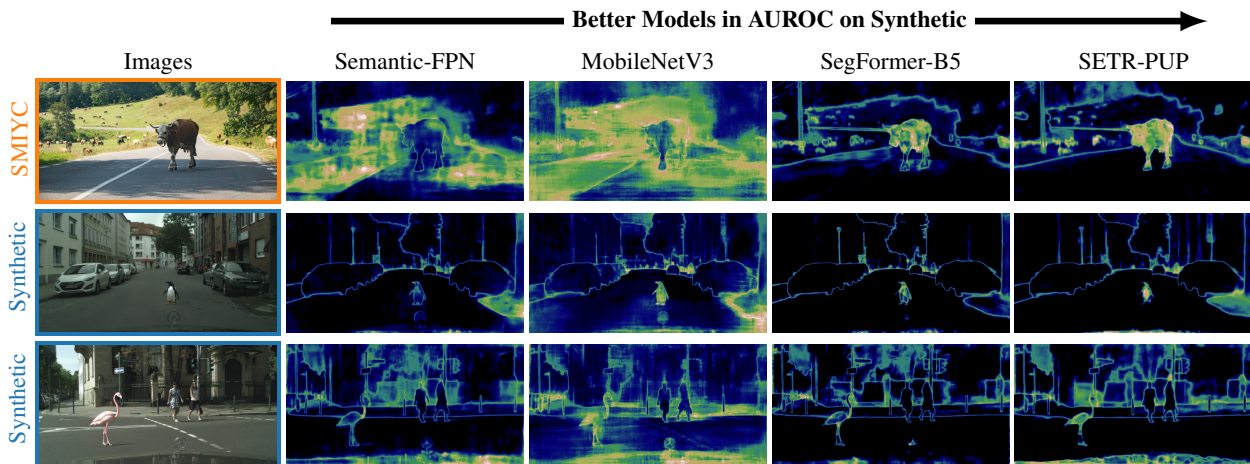


Figure 10. **Qualitative results.** Confidence maps are visualized for the four exemplified models on real data (first row) and synthetic inpainted data (second and third rows). Hotter colors correspond to higher OOD likelihood. Ideally, results should exhibit hot colors in OOD areas and cold colors everywhere else. We observe a strong correlation in model reactions to real and synthetic OOD regions, particularly for more recent and robust models.

proving OOD detection. To this end, we construct two different sets: (i) all 23,040 images generated automatically and (ii) 656 curated images where we manually select the best images in terms of visual quality and realism. We note that the manual selection process for the curated set is not exhaustive and is constrained by our allocated resources; there are many more high-quality images in the ‘all’ set. In what follows, we present results using both curated and uncurated sets.

4.2. Assess OOD Detection

Experimental setup. To measure how the segmenters react to unseen OOD objects, we use standard anomaly detec-

tion metrics [36], that are False Positive Rate at 95% true positives (FPR_{95}), Area Under ROC curve (AUROC), and Area Under Precision-Recall curve (AUPR). AUPR are declined into $AUPR_{IN}$ and $AUPR_{OUT}$, that considers the in-distribution regions, respectively the out-of-distribution regions (the inpainted object), as positive regions to compute the Precision-Recall curves.

All segmenters in our study are not designed to produce confidence scores. We thus seek for various techniques to derive confidence scores from pretrained models [12] and eventually narrow down the options to two measures: (i) Entropy of soft-probability predictions, and (ii) MaxLogit as the maximum logit value (before softmax) among the

Method	AUROC (\uparrow)	AUPR (\uparrow)	FPR95 (\downarrow)
RbA [22] Swin-B	95.6	78.4	11.8
+ COCO [22]	97.8	85.3	8.5
+ Ours (curated)	97.2	<u>84.9</u>	8.1
+ Ours (all)	<u>97.3</u>	84.8	<u>8.2</u>
RbA [22] Swin-L	96.4	79.6	15.0
+ COCO [22]	98.2	88.7	<u>8.2</u>
+ Ours (curated)	97.2	88.0	7.9
+ Ours (all)	<u>98.1</u>	<u>88.6</u>	8.3

Table 1. **Improving OOD detection** on real SMIYC benchmarking using our synthetic data. All results are obtained using the published code and default parameters.

classes. While Entropy is the traditional measure of uncertainty, MaxLogit is a recent and surprising finding that has been proven to be more effective in estimating OOD confidence [12].

Results. For quantitative comparison, we leverage the SegmentMeIfYouCan (SMIYC) dataset [4], a recent dataset for OOD detection. We resort to the RoadAnomaly21 split in SMIYC, due to similarity in object scales to our synthetic data. We analyze the correlation between the OOD scores obtained on RoadAnomaly21 and one using our synthetic inpainted data. Figure 8 reports our first analysis on the entropy in the OOD areas, either real (RoadAnomaly21) or generated. For each model, we compute the Pearson Correlation (PCC) between real-OOD entropy and synthetic-OOD entropy; the computation is done on both ‘curated’ and ‘all’ sets. In terms of entropy, we observe a very high correlation between real- and synthetic-OOD, reaching 0.94 PCC using both ‘curated’ and ‘all’ sets.

We then analyze the correlation between real and synthetic anomaly metrics. Figure 9 presents our primary findings and Figure 10 illustrates some qualitative results. We observe a strong correlation with real scores when utilizing the ‘curated’ set for computing synthetic scores; the curated PCCs (■) are consistently around 0.8 across multiple metrics, irrespective of the two confidence measures. Although the correlations are somewhat weaker when using all uncurated synthetic data (□), such results remain acceptable, particularly when no effort is dedicated to curation.

Our results validate the potential of utilizing realistic synthetic data, inpainted with anomaly objects, for assessing OOD detection. In OOD testing, it is quite important to use high-quality synthetic inpainted data. Nonetheless, even non-curated synthetic data can offer an acceptable estimation of real performance with minimal curation costs.

4.3. Improve OOD Detection

In this experiment, we investigate if synthetic inpainted data can be used to enhance a deep network’s ability to detect OOD objects. To this end, we adopt the state-of-the-art

RbA [22] approach for OOD detection and train RbA models on our synthetic data.

OOD metrics are computed on RoadAnomaly21 and reported in Table 1. The RbA models trained on our data significantly outperform the vanilla RbA model. We reach comparable performance to the RbA variants that leverage the external COCO dataset for augmentation. Notably, there are no clear differences between using ‘curated’ or ‘all’ sets. *We conjecture that, unlike benchmarking, training for OOD detection does not demand a high degree of realism from synthetic data.* This explains why the simple strategy of copy-pasting COCO objects already proves effective. All results are consistent across the two addressed backbones. Figure 10 illustrates a few qualitative results.

5. Takeaways

In this work, we explore the potential of synthetic data in reliability assessment for semantic segmentation networks. Our promising results encourage further collective investigations into this research problem, paving the way for synthetic system validation, especially in safety-critical applications. We summarize here our primary findings:

- ▷ *Reliability Under Covariate Shifts:* synthetic data can help assess the relative robustness of models in real-life covariate shifts, especially useful when shifts to the training condition are significant. Synthetic data can well complement real data in system validation, helping reduce the total operational cost. Pretrained models can be calibrated using synthetic data to better estimate prediction confidence in any shifted domains.
- ▷ *Reliability Against OOD Objects:* synthetic data is useful in both OOD testing and OOD training; however, the demands on synthetic data quality differ in these two cases. In OOD testing, the best result estimations are obtained with the most realistically inpainted data, which may require a certain amount of curation time for qualitative assessment. The curation task is not time-demanding and can be done quickly with a reasonable budget. On the other hand, for OOD training, no curation is actually needed to achieve improvements.

Limitations. We focus our research on the task of semantic segmentation while keeping open the extension possibility to other critical tasks, such as object detection. Our quantitative assessments are confined to existing publicly available datasets. However, our framework is fully zero-shot and can be applied to any domain of interest. On the generative side, our study is restricted to Stable Diffusion and ControlNet due to our resource constraints. Of note, although improvements in this area should enhance the results, similar insights are expected to be achieved.

Acknowledgements. This work is supported by ELSA - European Lighthouse on Secure and Safe AI funded by the European Union under grant agreement No. 101070617. We thank the authors of RELIS [5] for providing us their pretrained checkpoints.

References

- [1] clip-interrogator. <https://github.com/pharmapsychotic/clip-interrogator>, 2023. 3
- [2] Victor Besnier, Himalaya Jain, Andrei Bursuc, Matthieu Cord, and Patrick Pérez. This dataset does not exist: training models from generated images. In *ICASSP*, 2020. 2
- [3] Hermann Blum, Paul-Edouard Sarlin, Juan Nieto, Roland Siegwart, and Cesar Cadena. The fishyscapes benchmark: Measuring blind spots in semantic segmentation. 2021. 2
- [4] Robin Chan, Krzysztof Lis, Svenja Uhlemeyer, Hermann Blum, Sina Honari, Roland Siegwart, Pascal Fua, Mathieu Salzmann, and Matthias Rottmann. Segmentmeifyoucan: A benchmark for anomaly segmentation. In *NeurIPS*, 2021. 2, 8
- [5] Pau de Jorge, Riccardo Volpi, Philip HS Torr, and Grégory Rogez. Reliability in semantic segmentation: Are we on the right track? In *CVPR*, 2023. 2, 4, 5, 9
- [6] Robert Geirhos, Kantharaju Narayanappa, Benjamin Mitzkus, Tizian Thieringer, Matthias Bethge, Felix A Wichmann, and Wieland Brendel. Partial success in closing the gap between human and machine vision. *NeurIPS*, 2021. 2
- [7] Chuan Guo, Geoff Pleiss, Yu Sun, and Kilian Q Weinberger. On calibration of modern neural networks. In *ICML*, 2017. 5
- [8] Ruifei He, Shuyang Sun, Xin Yu, Chuhui Xue, Wenqing Zhang, Philip Torr, Song Bai, and Xiaojuan Qi. Is synthetic data from generative models ready for image recognition? 2023. 2
- [9] Dan Hendrycks and Thomas Dietterich. Benchmarking neural network robustness to common corruptions and perturbations. In *ICLR*, 2019. 2
- [10] Dan Hendrycks and Kevin Gimpel. A baseline for detecting misclassified and out-of-distribution examples in neural networks. In *ICLR*, 2017. 1, 2
- [11] Dan Hendrycks, Steven Basart, Norman Mu, Saurav Kadavath, Frank Wang, Evan Dorundo, Rahul Desai, Tyler Zhu, Samyak Parajuli, Mike Guo, et al. The many faces of robustness: A critical analysis of out-of-distribution generalization. In *ICCV*, 2021. 1, 2
- [12] Dan Hendrycks, Steven Basart, Mantas Mazeika, Andy Zou, Joe Kwon, Mohammadreza Mostajabi, Jacob Steinhardt, and Dawn Song. Scaling out-of-distribution detection for real-world settings. In *ICML*, 2022. 2, 7, 8
- [13] Alexander Kirillov, Eric Mintun, Nikhila Ravi, Hanzi Mao, Chloe Rolland, Laura Gustafson, Tete Xiao, Spencer Whitehead, Alexander C. Berg, Wan-Yen Lo, Piotr Dollár, and Ross Girshick. Segment anything. *arXiv*, 2023. 6
- [14] Pang Wei Koh, Shiori Sagawa, Henrik Marklund, Sang Michael Xie, Marvin Zhang, Akshay Balsubramani, Weihua Hu, Michihiro Yasunaga, Richard Lanus Phillips, Irena Gao, et al. Wilds: A benchmark of in-the-wild distribution shifts. In *ICLR*, 2021. 1, 2
- [15] Guillaume Le Moing, Tuan-Hung Vu, Himalaya Jain, Patrick Pérez, and Matthieu Cord. Semantic palette: Guiding scene generation with class proportions. In *CVPR*, 2021. 2
- [16] Daiqing Li, Huan Ling, Seung Wook Kim, Karsten Kreis, Sanja Fidler, and Antonio Torralba. Bigdatasetgan: Synthesizing imagenet with pixel-wise annotations. In *CVPR*, 2022. 2
- [17] Xiaodan Li, Yuefeng Chen, Yao Zhu, Shuhui Wang, Rong Zhang, and Hui Xue. Imagenet-e: Benchmarking neural network robustness via attribute editing. In *CVPR*, 2023. 1, 3
- [18] Shilong Liu, Zhaoyang Zeng, Tianhe Ren, Feng Li, Hao Zhang, Jie Yang, Chunyuan Li, Jianwei Yang, Hang Su, Jun Zhu, et al. Grounding dino: Marrying dino with grounded pre-training for open-set object detection. *arXiv*, 2023. 6
- [19] Andreas Lugmayr, Martin Danelljan, Andrés Romero, Fisher Yu, Radu Timofte, and Luc Van Gool. Repaint: Inpainting using denoising diffusion probabilistic models. In *CVPR*, 2022. 6
- [20] Aboli Marathe, Deva Ramanan, Rahee Walambe, and Ketan Kotecha. Wedge: A multi-weather autonomous driving dataset built from generative vision-language models. In *CVPRW*, 2023. 2
- [21] John P Miller, Rohan Taori, Aditi Raghunathan, Shiori Sagawa, Pang Wei Koh, Vaishaal Shankar, Percy Liang, Yair Carmon, and Ludwig Schmidt. Accuracy on the line: on the strong correlation between out-of-distribution and in-distribution generalization. In *ICLR*, 2021. 2
- [22] Nazir Nayal, Misra Yavuz, Joao F Henriques, and Fatma Güney. Rba: Segmenting unknown regions rejected by all. In *ICCV*, 2023. 8, 11
- [23] Yaniv Ovadia, Emily Fertig, Jie Ren, Zachary Nado, David Sculley, Sebastian Nowozin, Joshua Dillon, Balaji Lakshminarayanan, and Jasper Snoek. Can you trust your model’s uncertainty? evaluating predictive uncertainty under dataset shift. *NeurIPS*, 2019. 1, 2
- [24] Peter Pinggera, Sebastian Ramos, Stefan Gehrig, Uwe Franke, Carsten Rother, and Rudolf Mester. Lost and found: detecting small road hazards for self-driving vehicles. In *IROS*, 2016. 2
- [25] Viraj Prabhu, Sriram Yenamandra, Prithvijit Chattopadhyay, and Judy Hoffman. Lance: Stress-testing visual models by generating language-guided counterfactual images. In *NeurIPS*, 2023. 1, 3
- [26] Benjamin Recht, Rebecca Roelofs, Ludwig Schmidt, and Vaishaal Shankar. Do imagenet classifiers generalize to imagenet? In *ICLR*, 2019. 1, 2
- [27] Robin Rombach, Andreas Blattmann, Dominik Lorenz,

- Patrick Esser, and Björn Ommer. High-resolution image synthesis with latent diffusion models. In *CVPR*, 2022. 1, 3
- [28] Christos Sakaridis, Dengxin Dai, and Luc Van Gool. Acdc: The adverse conditions dataset with correspondences for semantic driving scene understanding. In *ICCV*, 2021. 2, 3
- [29] Mert Bulent Sariyildiz, Karteek Alahari, Diane Larlus, and Yannis Kalantidis. Fake it till you make it: Learning transferable representations from synthetic imagenet clones. In *CVPR*, 2023. 2
- [30] Aaditya Singh, Kartik Sarangmath, Prithvijit Chattopadhyay, and Judy Hoffman. Benchmarking low-shot robustness to natural distribution shifts. In *ICCV*, 2023. 2
- [31] Rohan Taori, Achal Dave, Vaishaal Shankar, Nicholas Carlini, Benjamin Recht, and Ludwig Schmidt. Measuring robustness to natural distribution shifts in image classification. *NeurIPS*, 2020. 1, 2
- [32] Damien Teney, Yong Lin, Seong Joon Oh, and Ehsan Abbasnejad. Id and ood performance are sometimes inversely correlated on real-world datasets. *arXiv*, 2022. 2
- [33] Dustin Tran, Jeremiah Liu, Michael W Dusenberry, Du Phan, Mark Collier, Jie Ren, Kehang Han, Zi Wang, Zeldia Mariet, Huiyi Hu, et al. Plex: Towards reliability using pretrained large model extensions. *arXiv*, 2022. 1
- [34] Girish Varma, Anbumani Subramanian, Anoop Namboodiri, Manmohan Chandraker, and CV Jawahar. Idd: A dataset for exploring problems of autonomous navigation in unconstrained environments. In *WACV*, 2019. 3
- [35] Weijia Wu, Yuzhong Zhao, Mike Zheng Shou, Hong Zhou, and Chunhua Shen. Diffumask: Synthesizing images with pixel-level annotations for semantic segmentation using diffusion models. In *ICCV*, 2023. 2
- [36] Jingkang Yang, Pengyun Wang, Dejian Zou, Zitang Zhou, Kunyuan Ding, Wenxuan Peng, Haoqi Wang, Guangyao Chen, Bo Li, Yiyun Sun, et al. Openood: Benchmarking generalized out-of-distribution detection. *NeurIPS*, 2022. 1, 2, 7
- [37] Lvmin Zhang, Anyi Rao, and Maneesh Agrawala. Adding conditional control to text-to-image diffusion models. In *ICCV*, 2023. 3, 11
- [38] Yuxuan Zhang, Huan Ling, Jun Gao, Kangxue Yin, Jean-Francois Lafleche, Adela Barriuso, Antonio Torralba, and Sanja Fidler. Datasetgan: Efficient labeled data factory with minimal human effort. In *CVPR*, 2021. 2

Appendix

In this appendix, we provide technical details for covariate shifts generation and OOD object inpainting (Appendix A), additional calibration details and results (Appendix B), and more qualitative examples (Appendix C).

A. Technical Details

A.1. Covariate Shifts Training

We train a ControlNet on top of a frozen Stable Diffusion 1.5 for 2100 steps. The ControlNet used here is a trainable copy of the Stable Diffusion encoder only, as in the original paper [37]. We use a batch size of 8 with 32 gradient accumulation steps, which makes an effective batch size of 256, and a learning rate of 10^{-5} . We use the training set of Cityscapes, and do a random horizontal crop of the images to get square images, and then resize them to 512×512 , convenient of Stable Diffusion 1.5. All other training hyperparameters are the per default settings on the official ControlNet repository. The objective is to reconstruct the original images of Cityscapes using its semantic masks as input to the ControlNet, and the captions extracted with CLIP-interrogator as input to Stable Diffusion.

A.2. Covariate Shifts Generation

To generate images with new styles, we take a semantic mask from the validation set of Cityscapes, crop and resize it as explained in the previous part. We use nearest neighbor interpolation to keep good values for specific classes. We only use the part of the caption extracted with CLIP-interrogator which corresponds to a BLIP caption. To this new caption, we add [, in <domain>] depending on the domain we want to generalize to. Starting from pure noise, we use 25 DDIM steps with a guidance scale of 8. On a RTX 2080, one new image is generated in about 4 seconds. All other sampling hyperparameters are the per default settings on the official ControlNet repository.

A.3. OOD Objects Generation

The OOD object generation pipeline described in Section 4.1 is further illustrated in Figure 11. It is composed of three steps. Given a text prompt containing an object, the inpainting step generates a zoomed-in version of the object with the appropriate close-range background given as context. The mask extraction step infers the anomaly mask from the zoomed-in generated image and the name of the object. Both are in-pasted back in the original complete image or mask. To reduce some composition artifacts, the composite image is refined with a noise/denoise step.

In details, we first randomly choose a box size for the new object, uniformly sampled between a quarter and half

the minimum dimension of the original image. We also uniformly sample a location for the box in the bottom three quarters of the image. This box will contain the new object we wish to add, and we refer to it as *inpainted region*. In addition to the inpainted region, we create a larger box, $1.5 \times$ its height and width, with the inpainted region in its center. The contour outside of the inpainted region will serve as *context* for the inpainting process. We then crop and resize the inpainted region with its context to a resolution of 512×512 . We fully noise the inpainted region, but leave the clean context. We then denoise the inpainted zone with the prompt “A photo of an [object]”, with a guidance scale of 15. The full patch is then resized and pasted on the original image, at its original position. Some artifact might be still present as shown in Figure 12. To remedy this, we refine the inpainted zone by noising and denoising it with 0.65 strength, with the default guidance scale of 7.5. The effect of this refining step is shown in Figure 12.

We list here all 42 objects used in our experiments, which are not present in Cityscapes’ classes: arcade machine, arm-chair, baby, bag, bathtub, bench, billboard, book, bottle, box, chair, cheetah, chimpanzee, clock, computer, desk, dolphin, elephant, flamingo, giraffe, gorilla, graffiti, hippopotamus, kangaroo, koala, lamp, lion, microwave, mirror, panda, penguin, pillow, plate, polar bear, radiator, refrigerator, sofa, table, tiger, toilet, vase, and zebra.

A.4. OOD Detection Training

For the OOD detection method in Section 4.3, we used the codebase of [22]. We adapt the code to be able to use our generated data with the binary masks extracted from Grounded-SAM, as explained in Section A.3. As in the original paper [22], we fine-tune the mask prediction MLP and classification layer after the transformer decoder. To obtain all results reported in Table 1, we used the recommended hyperparameters, and train the models for 5000 iterations.

A.5. Segmentation Models

We list here all models used in our experiments: ANN-R101, ANN-R50, APCNet-R101, APCNet-R50, BiSeNetV1-R50, BiSeNetV2-FCN, CCNet-R101, CCNet-R50, ConvNext, ConvNext-B-In1K, ConvNext-B-In21K, DLV3+ResNet101, DLV3+ResNet18, DLV3+ResNet50, GCNet-R101, GCNet-R50, ICNet-R101, ICNet-R18, ICNet-R50, MobileNetV3, PSPNet-R101, PSPNet-R18, PSPNet-R50, SETR-MLA, SETR-Naive, SETR-PUP, SegFormer-B0, SegFormer-B1, SegFormer-B2, SegFormer-B3, SegFormer-B4, SegFormer-B5, SegFormer-B5-v2, SegFormer-B5-v3, Segmenter, SemFPN-R101, SemFPN-R50, UpperNet-R101, UpperNet-R18, UpperNet-R50.

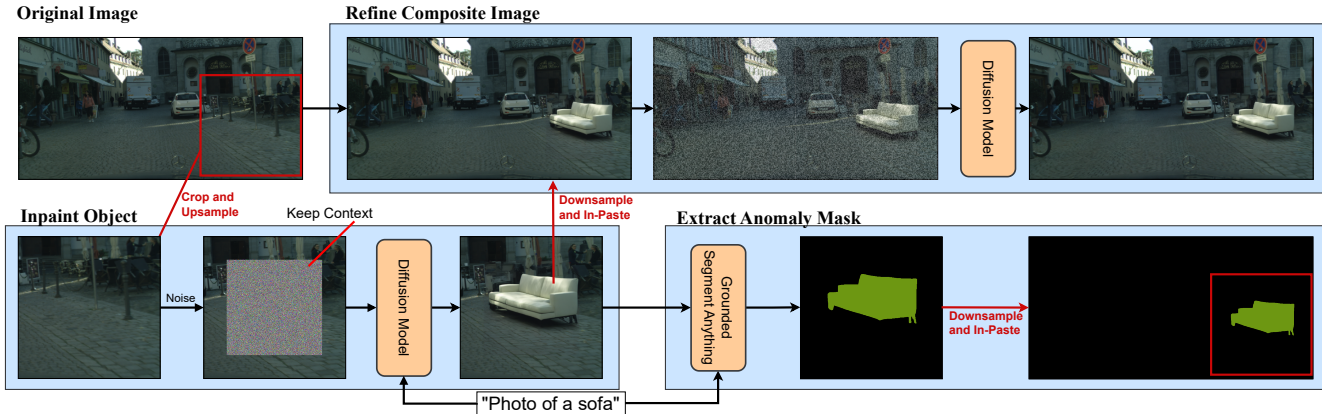


Figure 11. **OOD object data generation pipeline.** We use pretrained Stable Diffusion for inpainting and refining steps, and pretrained Grounded Segment Anything for mask extraction.

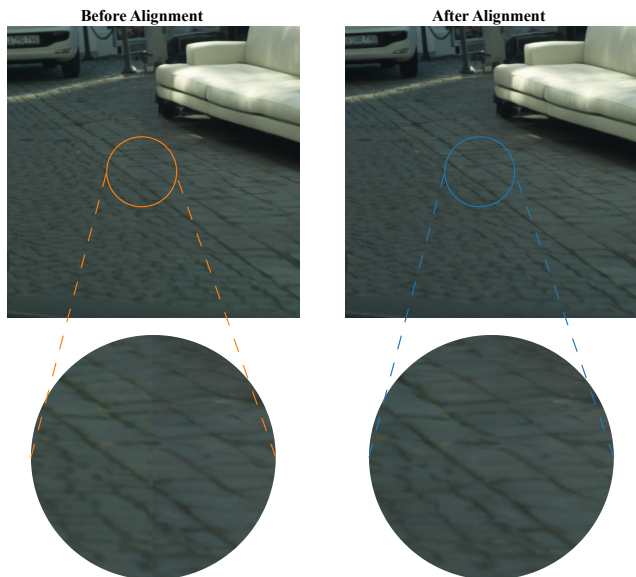


Figure 12. **Refinement.** This example highlights the importance of the refinement step. The left image shows the state before refinement, whereas the right image displays the refined version. Upon zooming into the edge of the inpainting box, a clear distinction between the left and right is evident in the first image. Such difference is eliminated in the second image. Must be viewed in color.

B. Calibration Details and Additional Results

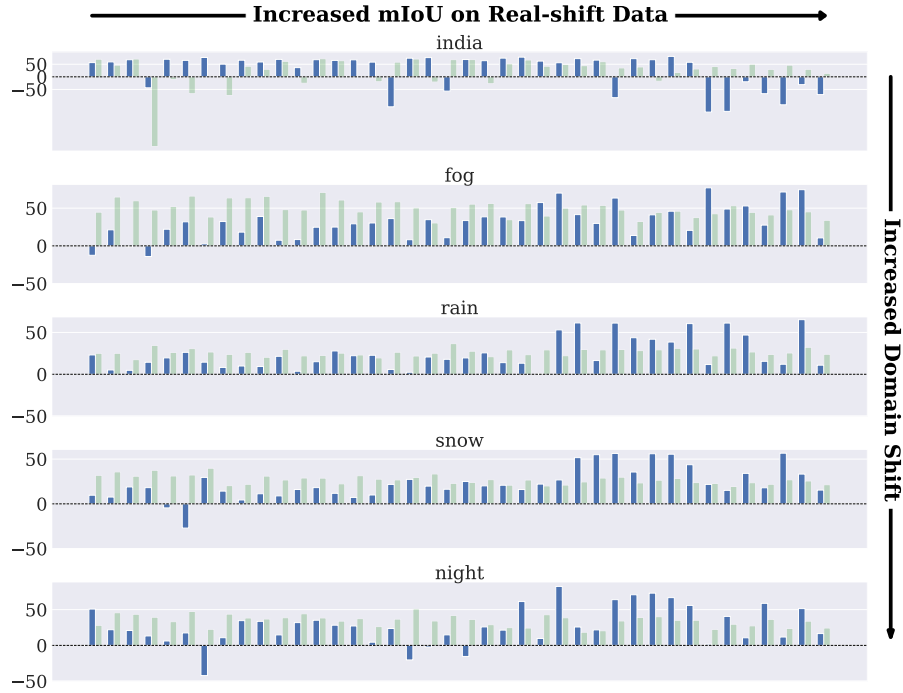
We elaborate on our strategy for performing per-class calibration to obtain the synthetic results (■) presented in Figure 6. Utilizing our synthetic data, a temperature scaling (TS) scalar is learned for each class. When calibrating models on shifted domains, we choose the corresponding TS scalar based on model predictions. In the case of calibration results with real-shift data (■), only one scalar is learned for each model.

In Figure 13a, we compare per-class TS *vs.* standard TS with one scalar per model, both applied on our synthetic data. Both strategies enhance calibration results, highlighting the advantage of employing synthetic data for calibration. Per-class TS demonstrates superiority for more robust models (right part of the plots), while its performance is weaker for less robust ones (left part of the plots).

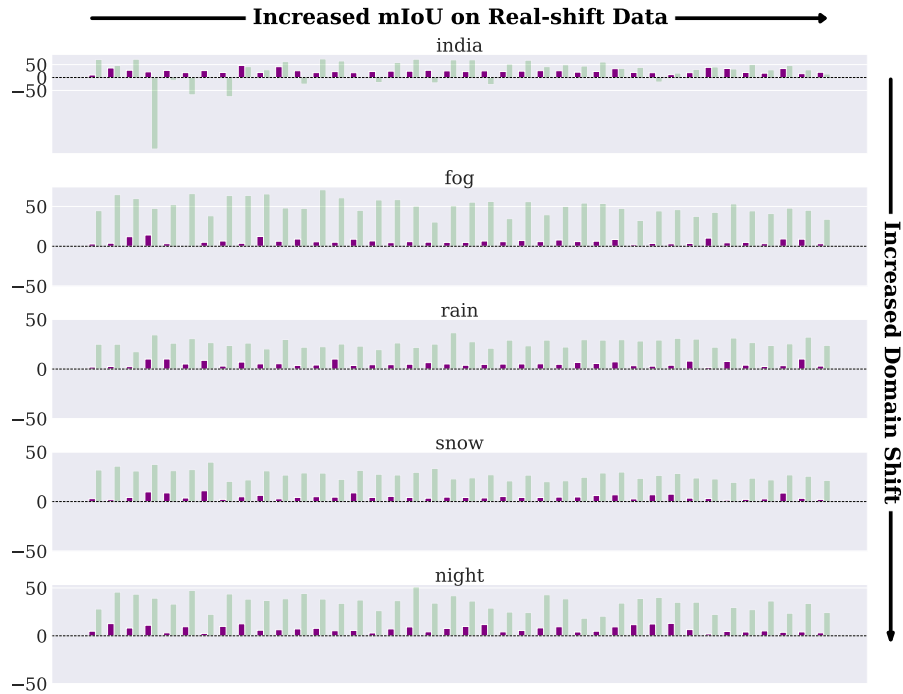
In Figure 13b, we compare Cityscapes *vs.* our synthetic data; in this experiment we adopt the standard TS with one scalar per model. The results obtained from Cityscapes are clearly inferior to those achieved using our synthetic data, demonstrating the limitations when relying solely on in-domain data for calibration in shifted domains.

C. Qualitative Examples

We show more qualitative examples for synthetic covariate shifts in Figure 14 and synthetic OOD objects in Figure 15.



(a) **Perclass Temperature Scaling (■) vs. One Temperature Scaling (■).** The Figure has the same structure as of Figure 6 and the bars show relative ECE improvements. We compare the two strategies for performing calibration using synthetic data; both enhance calibration in shifted domains.



(b) **Cityscapes (■) vs. our synthetic data with one TS (■).** The Figure has the same structure as of Figure 6 and the bars show relative ECE improvements. Our synthetic data is superior to Cityscapes in improving calibration in shifted domains.

Figure 13. **Additional Calibration Results.**



Figure 14. **Qualitative results.** Examples of rare conditions generated for testing and predictions from different models. Results of the strong model like SegFormer-B5 is visibly better than the Semantic-FPN and MobileNetV3.

